

A method for predicting condensation-driven heat removal in a BWR passive containment cooling system

Karen M. Vierow

*Nuclear Power Engineering Corporation, Fujita Kanko Toranomon Bldg. 5F,
3-17-1 Toranomon, Minato-ku, Tokyo, 105, Japan*

(Received August 1, 1994)

Passive designs of several proposed light water reactors rely on containment cooling by condensation heat transfer in a high-concentration, noncondensable gas environment. To evaluate the safety of these plants, methods for analyzing the performance of the cooling systems must be developed. The current study discusses the physics of condensation in the presence of noncondensable gases and a method for predicting the accompanying heat transfer rates based on experimental data. The resulting experimental correlation for heat transfer coefficients has been implemented into the TRACG code, and a specific application has been made to the Simplified Boiling Water Reactor for conditions following a Design Basis Accident LOCA (Loss-of-Coolant Accident)

1. INTRODUCTION

The reduction of condensation heat transfer due to the presence of a noncondensable gas is a critical consideration which must be incorporated into the design of heat exchangers where such gases are present. An example of an application is for the SBWR, for which long-term containment cooling depends on condenser heat exchangers located above the upper drywell region of the containment vessel. Following blowdown of the reactor vessel into the containment, the vertical tubes of the heat exchangers take in a mixture of steam and gases. Heat is removed from the containment vessel via steam condensation, however, the gases may impede the heat transfer process and result in unacceptable conditions in the containment.

The need for the current study arose from the lack of a method to accurately predict the SBWR containment cooling phenomena and insufficient knowledge of the physical processes occurring during condensation from a steam-noncondensable gas mixture. Early work on the condensation problem dealt with laminar film condensation of vapor from a stagnant gas mixture for natural convection on a vertical plate [7, 9]. Under such conditions, vapor carries gas towards the condensation surface. The gas accumulates, forming a high-concentration boundary layer along the condensing film. From thermodynamic considerations, the low vapor partial pressure near the wall results in a low vapor saturation temperature under equilibrium conditions. With the temperature difference which drives heat transfer between the vapor and condensation surface reduced, the condensation rate is lower than that for a pure vapor atmosphere. Conduction, convection and radiation heat transfer rates are also reduced, however, the current analysis focuses on the condensing mode.

In a similar manner, a noncondensable gas boundary layer forms along the inner surface of vertical heat exchanger tubes. The present problem differs in that the gas environment has a non-zero velocity and the composition of the vapor-gas mixture varies axially as well as radially. Earlier studies of forced convection condensation from a steam-noncondensable gas mixture have been performed [4, 5]. However, local data are needed for the present application and only tube-average results have been presented to date.

The TRACG code is used to evaluate the system behavior for decay heat removal following a Design Basis Accident LOCA. Several modifications were necessary to extend TRACG analysis capabilities, including a formulation for condensation heat transfer in the heat exchangers.

The present paper focuses on the development of a method for predicting local heat transfer rates. Specifically, the physics behind condensation in the presence of noncondensable gases are discussed and an experimental program which provided data for the development of a heat transfer coefficient correlation is described. An explanation is provided of the application for which the correlation was developed, namely the SBWR system, and the TRACG code. Finally, results of TRACG simulations are presented which show the containment behavior following a Design Basis Accident LOCA.

ACKNOWLEDGEMENTS

2. THEORY OF CONDENSATION WITH NONCONDENSABLE GASES PRESENT

As stated previously, studies on laminar film condensation of vapor from a gas mixture for natural convection on a vertical flat plate have been conducted. However, many practical situations, including the SBWR application, involve forced convection gas flow which introduces additional phenomena.

The physical situation inside a vertical tube is shown in Fig. 1. A steam-noncondensable gas mixture enters the condenser and vapor begins to condense at the inlet. As steam is drawn to the cooling surface, the gas experiences a force similar to suction through a permeable wall. The noncondensable gas concentration at the film interface becomes higher than that in the central core and a gas-vapor boundary layer develops adjacent to the liquid boundary layer. Between the annular gas boundary layer and tube centerline, the steam concentration is constant. However, the cross-section average of noncondensable gas concentration increases with distance along the tube axis as the boundary layer thickens. At some axial location, the boundary layer bridges the tube so that there is no longer a central core of inlet composition.

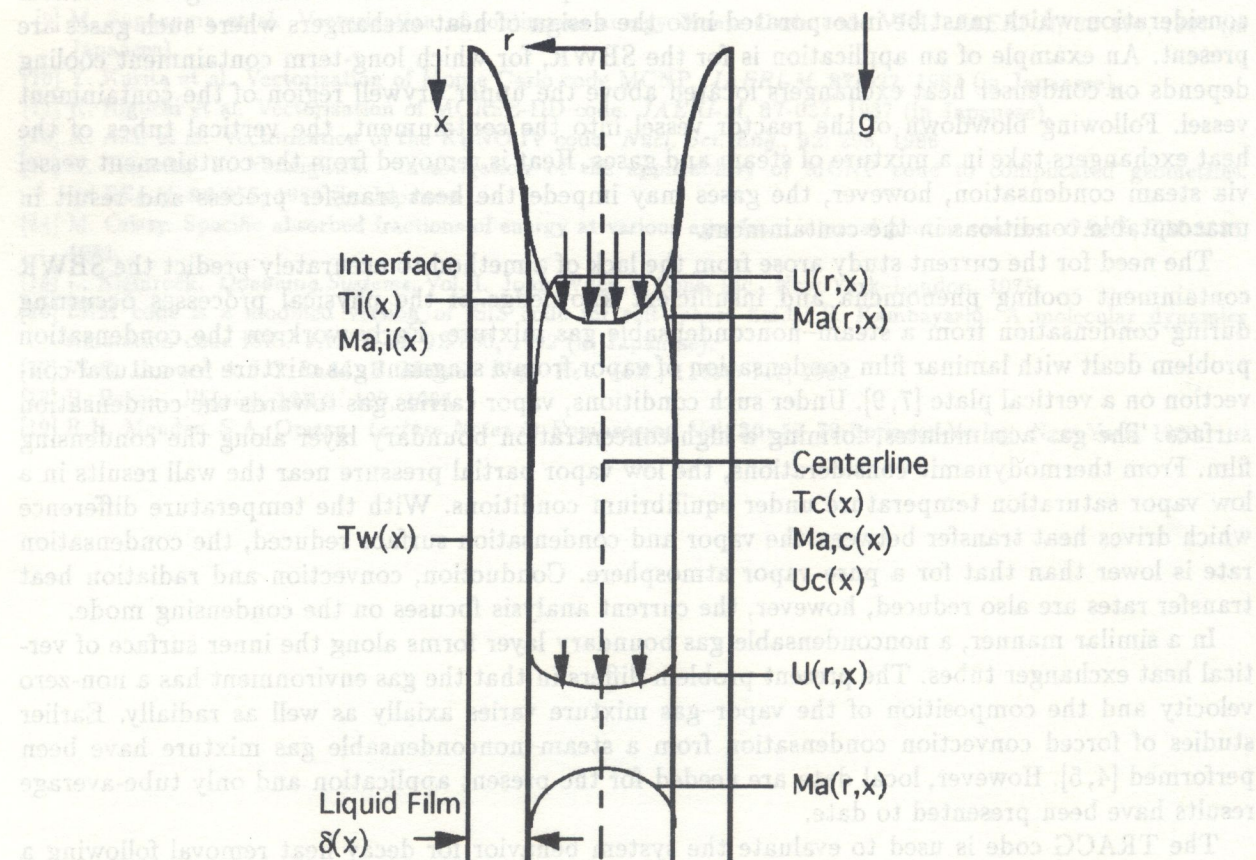


Fig. 1. Developing boundary layers

With steam continuing to condense, but at diminishing rates, a fully-developed condition may not be achieved in the gas phase. Downstream from the point of nearly complete condensation, the gaseous mixture contains steam in equilibrium with the condensate and noncondensable gas, with a partial pressure which maintains tube total pressure at nearly the system pressure level.

Another distinguishing feature of forced convection condensation inside tubes is the effect of interfacial shear. The gas phase has a higher velocity than the condensate film, producing interfacial shear and increasing condensate film turbulence. With the gas and liquid film both flowing downward, turbulence thins the film and reduces film resistance to heat transfer. Additionally, the increased interfacial shear promotes turbulence and mixing in the gas core. The resistance of the noncondensable gas boundary layer to condensation heat transfer is reduced. A third distinction concerns the axial variation of the cross-section average temperature and species concentration for the internal flow case. In contrast to the stagnant atmosphere case, the temperature decreases with distance along the condenser tube and the noncondensable gas concentration increases. Axial variations are produced in the conditions driving heat and mass transfer, but do not occur in the stagnant gas, vertical flat plate situation.

Sparrow's work [9] shows similarity in the boundary layers and a uniform interface temperature. For a constant, free stream gas mass fraction, Denny et. al. [6] note nonsimilarity in the three-phase problem. With a variable centerline gas mass fraction, the problem becomes even more nonsimilar in character. An exact analytical solution would require solving radially- and axially-dependent boundary layer conservation equations which could not be reduced to ordinary differential equations. A numerical solution is not attempted in this analysis.

3. EXPERIMENTAL PROGRAM

3.1. Facility description

A natural circulation closed loop was constructed to obtain experimental data for local heat transfer rate evaluation [10]. The closed loop consisted of a lower plenum, a vertical riser, the heat exchanger test section, and a downcomer which returned to the lower plenum. A steam injection connection and a condensate drain connection were made to the lower plenum. The entire system was insulated.

The vertical test section was a concentric tube, counterflow heat exchanger with steam condensing in the inner tube and coolant flowing up the secondary-side, annular cooling jacket. Steam and noncondensable gases entered from the top of the copper condenser tube, 0.022 mm inner diameter and 2.1 m in length, with liquid condensate and a gas mixture exiting via the downcomer. The coolant flow was maintained at a rate sufficient to condense nearly all of the primary-side steam, while enabling the measurement of an accurate secondary-side, axial temperature profile.

Instrumentation consisted of thermocouples, pressure transducers and flow meters around the system. The axial temperature profile of the condenser tube outer wall and coolant bulk temperature were measured to obtain local heat transfer data. Loop pressure and temperature values were also recorded and the coolant flow rate was measured with an orifice flow meter.

3.2. Test procedures

During the startup procedures, the closed loop was brought down to a vacuum, and then a measured amount of noncondensable gas was let into the system. (Air was used to simulate the nitrogen in the SBWR containment.) The mass of air remained constant throughout a single test, enabling determination of gas concentrations in the system under steady-state conditions. Steam was injected into the lower plenum where it mixed with the air. The air-vapor mixture circulated up the riser, through two 90° bends, and condensed in the test section. Condensate, and some gas mixture, returned to the lower plenum via the downcomer. Liquid condensate was drained so as to maintain a constant water level in the plenum.

The steady rate of steam supply was fixed by setting the boiler heater power to a pre-determined level. When at steady-state, the constant rate of the coolant flow was measured with an orifice flow meter and the constant condensate drainage rate was recorded.

When all temperatures, pressures and flow rates were constant for at least ten minutes, a steady state was considered to exist. At this point, steady-state data was recorded. Heat balances were performed to ensure that all of the energy in the system could be accounted for. Leakage tests were conducted prior to each test to ensure that no loss or gain of noncondensable gas occurred during a test.

The range of test conditions, shown in Table 1, was specified so as to cover the expected conditions in the SBWR heat exchangers.

Table 1. Range of operating parameters

Parameter	Operating range
Heater power	6–18.9 kW
Vapor flow rate	5.9–25 kg/h
System pressure	30–452 kPa
System temperature	72–146°C
Coolant inlet temperature	9–12°C
Coolant outlet temperature	17–23°C
Coolant flow rate	364–1432 kg/h
Inlet air mass fraction	0.0–0.14

3.3. Correction factor

The heat flux decreased with distance along the condenser from a maximum value at the inlet. The air mass fraction gradually increased, and the gas mixture Reynolds number decreased, before rapidly changing to nearly 1.0 and 0.0 respectively at the end of the condensation zone. In these experiments, the end of the condensing zone was observed to be between 0.4 m and 1.25 m. In the lower region of the tube, the amount of condensation heat transfer was negligible. The local gas mixture was saturated at nearly the local coolant temperature. The local partial pressure of steam corresponded to the steam saturation pressure at the local temperature, both of which were low values.

The data were used to obtain local condensation heat transfer coefficients. To evaluate the air mass fraction at the condenser entrance, the air mass in the condenser and downcomer was found from approximate calculations. The total amount of air in the system was known and the amount not in the condenser or downcomer was assumed to be uniformly distributed throughout the rest of the loop. Axial profiles of the tube wall and secondary-side fluid temperatures, bulk air mass fraction in the condenser tube, bulk gas–vapor mixture Reynolds number, condensate flow rate and other parameters were obtained.

Based on these data, a correction factor, in the form of a multiplier to the pure steam Nusselt heat transfer coefficient, has been developed [12]. The Nusselt theory heat transfer coefficient was calculated as liquid thermal conductivity divided by the local liquid film thickness, where the liquid film was assumed to be laminar and not experiencing interfacial shear. This condensate film thickness was only used as a basis for calculations and may have differed from the actual film thickness. The local liquid flow rate was determined with the use of an energy balance on a control volume spanning the tube inlet to the current location.

The correction factor to the Nusselt heat transfer coefficient accounts for the effects of the local noncondensable gas mass fraction and the local gas mixture flow rate. This local heat transfer

coefficient is expressed as:

$$h(x) = h_{Nu}(x) \cdot f(x) \quad (1)$$

$$f(x) = \left[1 + 2.88 \cdot 10^{-5} Re_{mix}(x)^{1.18} \right] \cdot \left[1 - C M_a(x)^b \right] \quad (2)$$

where:

$$C = 10.0 \quad b = 1.0 \quad M_a < 0.063$$

$$C = 0.938 \quad b = 0.13 \quad 0.063 < M_a < 0.60$$

$$C = 1.0 \quad b = 0.22 \quad 0.60 < M_a$$

The correction factor, $f(x)$, accounts for two opposing effects. The first term in Eq. 2 incorporates the effect of interfacial shear from the higher velocity gas mixture on the lower velocity condensate film, which promotes condensation heat transfer. As the mixture Reynolds number approaches zero, the first term reaches the appropriate limit of one (no enhancement due to shear). The second term decreases the correction factor with increasing noncondensable gas mass fraction, due to the additional gas thermal resistance not present in the pure steam Nusselt theory situation. This term approaches the bounding value of zero as the noncondensable gas mass fraction approaches one, and the limit of one in the pure steam situation. Near the tube inlet, the enhancement effects of convective shear may dominate over the degradation effects of the noncondensable gases and cause the correction factor to exceed unity. Since the correlation yields large values at very low mass fractions and high mixture Reynolds numbers, an engineering judgement was made to impose an upper limit on the first term of Eq. 2 in the analysis methods. A value of 3.0 was deemed appropriate because the experimental data was limited in the high Reynolds number range.

4. SBWR DESCRIPTION

A condensation heat transfer mechanism of long-term decay heat removal, the Passive Containment Cooling System (PCCS), has been incorporated into the design of the Simplified Boiling Water Reactor [11, 13]. Accurate modeling of PCCS heat transfer for safety analyses required experimental simulation to determine local heat transfer rates. The previously described experimental program was initiated specifically for application to the SBWR.

The PCCS is a post-LOCA, low pressure, decay heat removal system designed for the SBWR. Its function is to remove heat from the reactor containment system (drywell and suppression chamber) and maintain pressure below the design value by passive means. The primary components of the PCCS are three condensation heat exchanger units. Located in a large pool of water outside of the containment, the PCCS units consist of an upper steam plenum, condenser tubes, and a lower condensate plenum (Fig. 2).

On the primary side of the PCCS units, noncondensable gases and decay heat steam enter from the drywell. Steam condenses inside the tubes and condensate drains to the GDCS pools. These pools are elevated relative to the reactor and serve to maintain reactor water inventory following an emergency depressurization of the primary system. These pools drain to the reactor pressure vessel when the sum of drywell pressure plus water head in the drain lines is greater than the sum of the reactor vessel pressure plus vessel water head above the drain line inlet nozzles. As the condensation proceeds, gases and a small amount of steam exiting the condenser tubes are vented to the suppression pool. The steam, drain, and vent flows are driven by natural circulation and the pressure difference between the drywell and the suppression chamber.

On the secondary side of the PCCS units, heat is carried away from the condenser tubes by water in the surrounding natural circulation pools. The pool water inventory is maintained sufficient to prevent tube uncover for at least seventy-two hours. The pool initially is subcooled at atmospheric pressure, and rises to saturation temperature at just above one atmosphere after a few hours of decay heat removal.

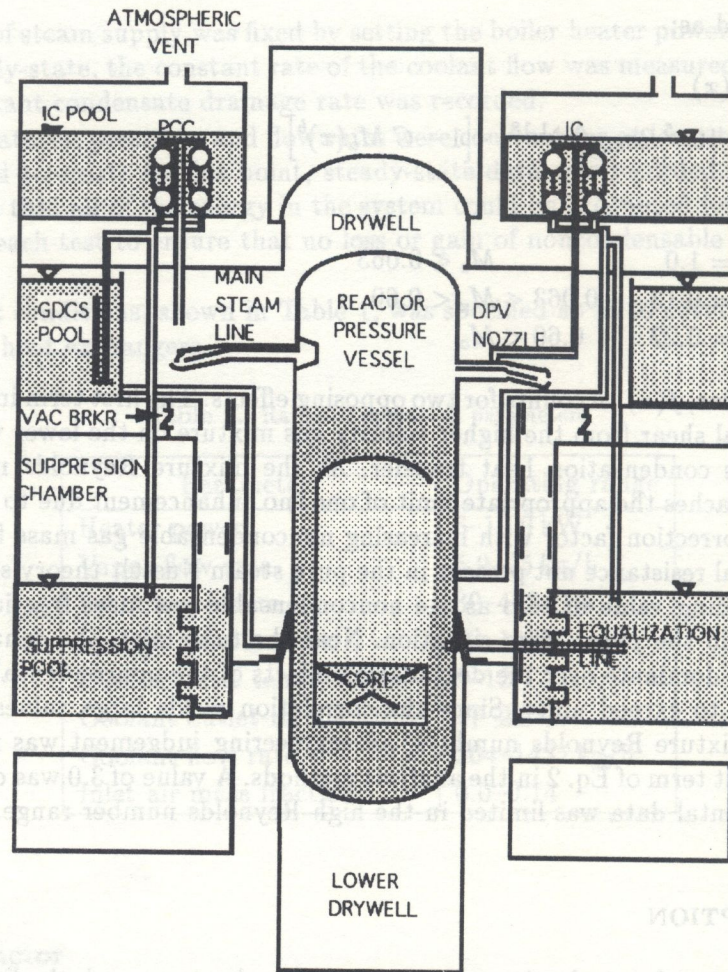


Fig. 2. SBWR containment cooling system

The distribution of noncondensable gases throughout the containment system is a key factor in determining the post-LOCA conditions and behavior of the PCCS units. During normal reactor operation, the SBWR containment is inerted with nitrogen, and operates at just above atmospheric pressure. The containment gas mixture is composed primarily of nitrogen and steam with a 29:1 partial pressure ratio in the drywell (20% humidity), and a 15:1 ratio in the suppression chamber (100% humidity). The low oxygen content prevents the buildup of a potentially combustible gas mixture. The noncondensable gas inventory has the potential to degrade the performance of the heat exchangers and the nitrogen partial pressure represents an increasingly significant portion of the total containment pressure as it concentrates in the suppression chamber following a blowdown.

Early in the blowdown transient, most of the drywell gas is transferred to the suppression chamber gas space, along with the blowdown steam, via the main drywell-to-suppression chamber vent system. The transferred quantity of noncondensable gases determines the gas partial pressure in the suppression chamber, and the amount of steam condensed in the suppression pool determines the post-blowdown pool liquid temperature and the suppression chamber vapor pressure. A large amount of steam carryover can significantly raise the suppression chamber vapor pressure and increase the overall containment pressure. The containment pressure would be increased less if the steam had instead condensed in the PCCS units. However, the PCCS was designed for long-term heat removal and does not have the capacity to remove all of the blowdown heat. In the longer term, residual noncondensable gas in the drywell is vented to the suppression pool via the PCCS units and, in the process, degrades heat removal performance by inhibiting steam condensation within the tubes.

5. THE TRACG CODE

TRACG, a GE version of the thermal-hydraulic computer code TRAC, is used to evaluate the system behavior for long-term decay heat removal following a LOCA. It is a "best estimate" computer code, applicable for the calculation of thermal hydraulic parameters and reactor power during BWR transients and postulated design basis accidents [2, 3]. TRAC includes capability for two or three-dimensional hydrodynamics calculations in regions representing the reactor vessel and containment volumes. Previous versions of TRACG have been qualified against separate-effects tests and integral tests representative of the BWR and SBWR [1]. This qualification covers blowdowns from high pressure and ensures accurate prediction of pressure, blowdown flow, and early containment response following LOCA's in the SBWR.

For the present application, the capabilities of TRACG were extended to include a heat transfer model for condensation in the presence of noncondensable gases and a number of refinements required to simulate long-term containment cooling behavior. Condensation phenomena in the vertical tube heat exchangers must be accurately modeled in order to predict the PCCS heat removal rates which characterize the post-accident behavior of the SBWR containment system. The experimental correlation for the correction factor to the Nusselt heat transfer coefficient was implemented to enable such calculations.

TRACG simulations of condensation heat transfer experiments in the JAPC/Toshiba full-height three-PCCS-tube integrated system test facility [8] were subsequently performed. The code predictions compared well with the system test results and validated the condensation heat transfer model for prediction of SBWR containment post-LOCA performance.

6. ANALYSIS OF THE SBWR PCCS

6.1. Model nodalization

The nodalization of the TRACG model for the SBWR containment is shown in Fig. 3 [11]. Its fundamental structure is an axisymmetric VSSL component with eight axial levels and five radial rings. The two innermost rings represent the chimney and downcomer regions of the reactor pressure vessel and the third ring represents the drywell. The first five axial levels of rings 4 and 5 represent the suppression pool and suppression chamber gas space. The upper three levels of rings 4 and 5 represent the drywell head and GDCS pool region, respectively. Energy input to the reactor pressure vessel fluid (decay heat plus stored energy released from reactor pressure vessel structures) is simulated by the CHAN08 component, located at approximately the elevation of the core.

The PCCS units are modeled by a set of components as shown. The PCCS heat transfer surface was divided into eight axial cells with a secondary-side heat sink temperature set at the saturation temperature in the water surrounding each cell. High pressure Isolation Condensers are also included in the model, however these components are valved off for the present analysis. The remaining model components represent the pipes and valves which connect the reactor pressure vessel, drywell, suppression chamber, GDCS, and PCCS. The VLVE18 component represents a postulated vapor/gas leakage path between the drywell and the suppression chamber gas space.

An additional feature of the model is the presence of heat conducting walls in level 5 between the drywell and the suppression chamber and between the suppression chamber and the model exterior. The drywell-suppression chamber wall is a carbon steel conductor which represents various pathways for heat flow through the vent wall and the concrete and steel girder ceiling of the suppression chamber. The outer wall is concrete and represents the portion of the containment pressure boundary adjacent to the suppression chamber gas space. It serves as a long-term heat sink for energy conducted or convected into the suppression chamber.

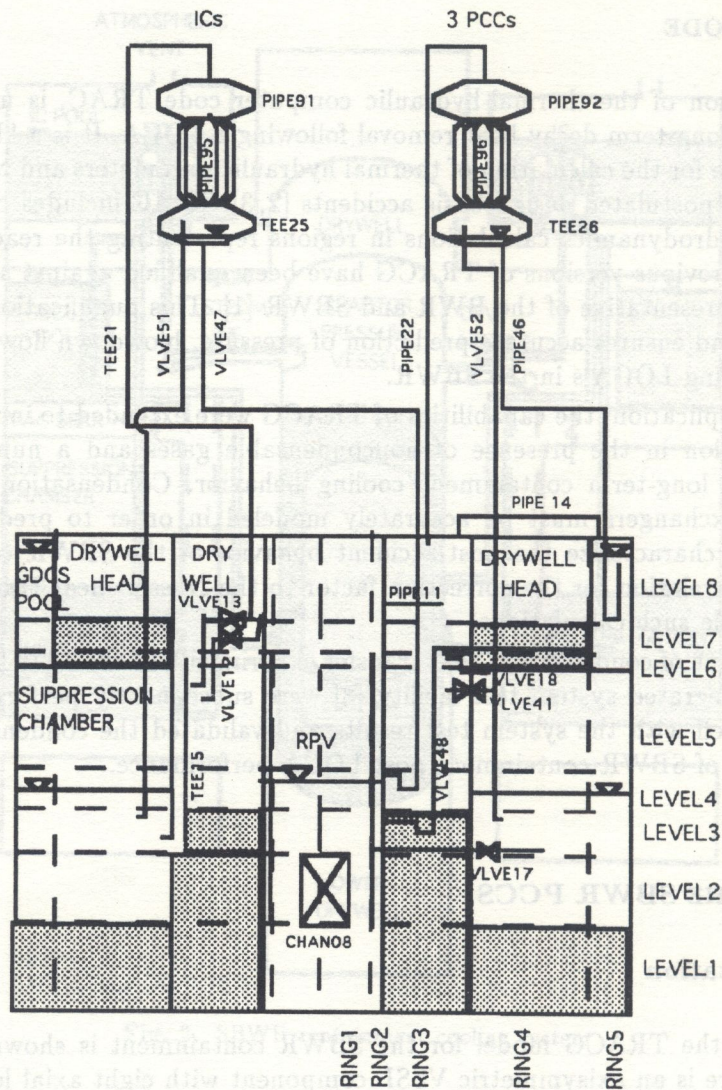


Fig. 3. TRACG SBWR model

6.2. Initial conditions

The 72-hour containment cooling transient following a main steam line break LOCA is analyzed herein. The start of the long-term cooling period (end of blowdown) is defined as the time at which GDCS injection to the reactor vessel begins. This time was calculated by a separate TRACG simulation with a detailed reactor pressure vessel model that accurately simulates loss of vessel inventory and operation of the systems which ensure rapid vessel depressurization. The time of GDCS injection is about 515 seconds after the break occurs. By this time, the reactor vessel and drywell pressures have equalized and the difference between the drywell and suppression chamber pressures corresponds to the submergence of the top main LOCA vent. The system is in a quasi-steady state from which an appropriate set of initial conditions for the long-term analysis is obtained.

6.3. Results of TRACG calculation

Results are shown in Figs. 4 through 6. The design requirement for the SBWR is that the PCCS must be able to remove decay heat and maintain containment pressure below 483 kPa (55 psig) for at least 72 hours with only simple operator actions and no benefit from active equipment. The calculations show that the units are able to fulfill this requirement.

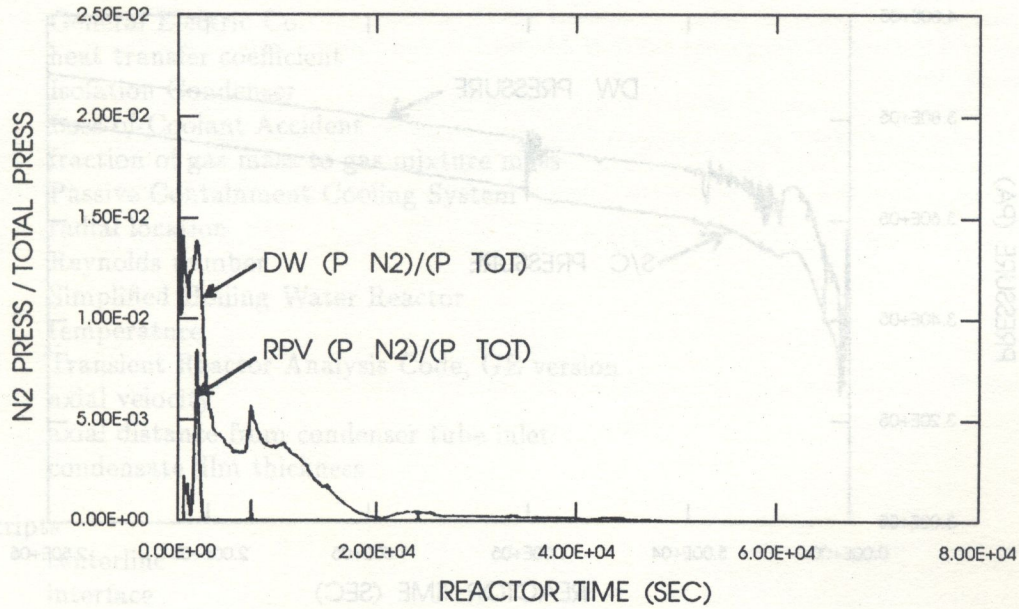


Fig. 4. N₂ condensation

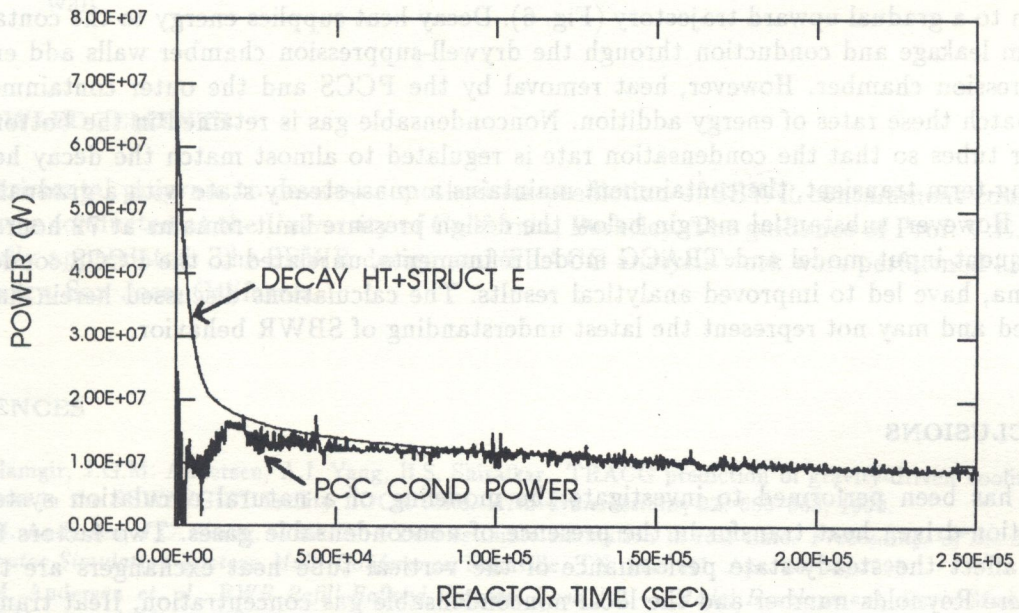


Fig. 5. Condenser heat removal

Figure 4 shows the variation in drywell nitrogen inventory over the first few hours of the transient. Most of the residual drywell inventory is quickly purged to the suppression chamber via the LOCA and PCCS vent lines. The drywell nitrogen inventory then increases as cold GDCS water enters the reactor pressure vessel and absorbs decay energy. As the GDCS flow decays, the PCCS must remove the decay heat and nitrogen is again purged to the suppression chamber.

Radiolytic gases generated in the reactor vessel are modeled in TRACG by an equivalent number of moles of nitrogen. The gas concentration in the reactor vessel is shown in Fig. 4. The spike in reactor vessel concentration early in the transient is caused by the GDCS cooling, which nearly suppresses steaming out of the reactor vessel.

Figure 5 compares PCCS heat removal with the system heat input for the entire 72-hour period. After a period of rising pressure, during which remaining noncondensable gas is purged from the drywell, the PCCS heat removal rate almost matches the decay heat rate and the pressure makes the

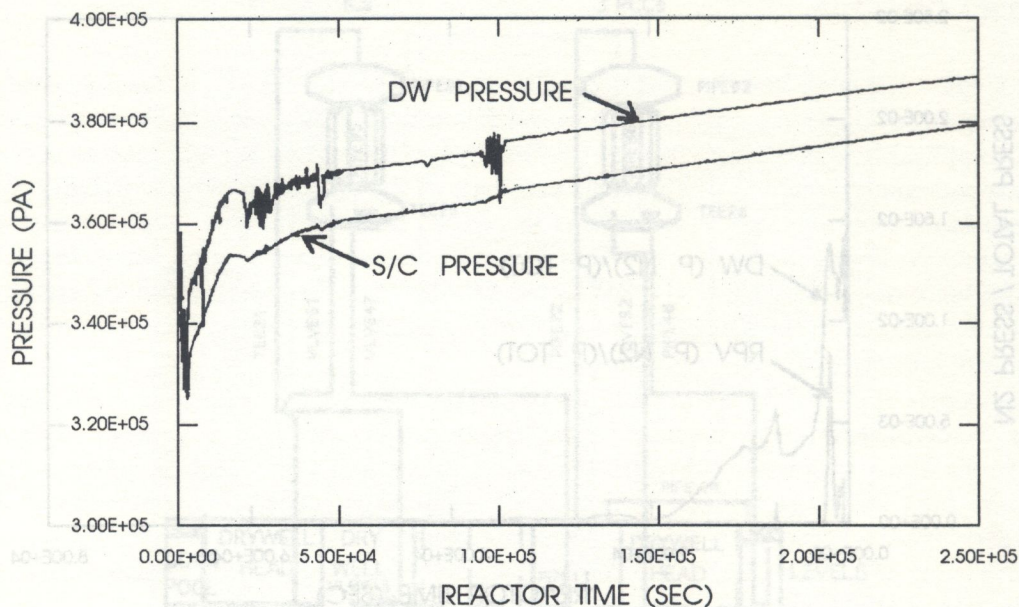


Fig. 6. Pressure

transition to a gradual upward trajectory (Fig. 6). Decay heat supplies energy to the containment, and steam leakage and conduction through the drywell-suppression chamber walls add energy to the suppression chamber. However, heat removal by the PCCS and the outer containment wall almost match these rates of energy addition. Noncondensable gas is retained in the bottom of the condenser tubes so that the condensation rate is regulated to almost match the decay heat rate. In the long-term transient, the containment maintains a quasi-steady state with a gradually rising pressure. However, substantial margin below the design pressure limit remains at 72 hours.

Subsequent input model and TRACG model refinements, unrelated to the PCCS condensation phenomena, have led to improved analytical results. The calculations discussed herein have been superseded and may not represent the latest understanding of SBWR behavior.

7. CONCLUSIONS

A study has been performed to investigate the modeling of a natural circulation system with condensation-driven heat transfer in the presence of noncondensable gases. Two factors found to strongly affect the steady-state performance of the vertical tube heat exchangers are the local gas mixture Reynolds number and the local noncondensable gas concentration. Heat transfer was enhanced by an increasing mixture Reynolds number (interfacial shear effect) and degraded by an increasing bulk air mass fraction (added thermal resistance effect).

A correlation for local heat transfer coefficients was developed and incorporated into the TRACG code. This correlation compared well with available experimental data and is currently used for analyzing the SBWR PCCS. Results of TRACG calculations indicate that the PCCS will perform satisfactorily to remove heat from the containment following a Design Basis Accident LOCA.

NOMENCLATURE

BWR	Boiling Water Reactor
DPV	Depressurization valve
f	heat transfer coefficient correction factor
g	gravity
GDCS	Gravity-Driven Cooling System

GE	General Electric Co.
h	heat transfer coefficient
IC	Isolation Condenser
LOCA	Loss-of-Coolant Accident
M_a	fraction of gas mass to gas mixture mass
PCCS	Passive Containment Cooling System
r	radial location
Re	Reynolds number
SBWR	Simplified Boiling Water Reactor
T	temperature
TRACG	Transient Reactor Analysis Code, GE version
U	axial velocity
x	axial distance from condenser tube inlet
δ	condensate film thickness

Subscripts

c	centerline
i	interface
mix	mixture
Nu	Nusselt
w	wall

ACKNOWLEDGEMENTS

The experimental program to develop a method for prediction of SBWR containment cooling phenomena was conducted at the University of California, Berkeley. The guidance of Prof. V.E. Schrock is gratefully appreciated. The SBWR design and TRACG analysis work were performed at GE Nuclear Energy, San Jose, California.

REFERENCES

- [1] M. Alamgir, J.G.M. Andersen, A.I. Yang, B.S. Shiralkar. TRACG prediction of gravity-driven cooling system response in the SBWR/GIST facility LOCA tests. *ANS Transactions*, **62**: 665-668, 1990.
- [2] J.G.M. Andersen, J.C. Shaug. TRACS — best estimate simulation in real time. *Proceedings of the Society for Computer Simulation Eastern Multi Conference*, Nashville, TN, 143-141, Apr. 23-26, 1990.
- [3] J.G.M. Andersen et al. *BWR Refill-Reflood Program Task 4.7 — Model Development, Basic Models for the BWR Version of TRAC*, GEAD-22051, NUREG/CR-2573, EPRI NP-2375, GE Nuclear Energy, San Jose, CA, Apr. 1990.
- [4] V.M. Borishanskiy et al. Heat transfer from steam condensing inside vertical pipes and coils. *Heat Transfer — Soviet Research*, **10**: 44-57, 1978.
- [5] V.M. Borishanskiy et al. Effect of uncondensable gas content on heat transfer in steam condensation in a vertical tube. *Heat Transfer — Soviet Research*, **9**: 35-42, 1977.
- [6] V.E. Denny, A.F. Mills, V.J. Jusonis. Laminar film condensation from a steam-air mixture undergoing forced flow down a vertical surface. *Journal of Heat Transfer*, 297-304, 1971.
- [7] W.J. Minkowycz, E.M. Sparrow. Condensation heat transfer in the presence of noncondensables, interfacial resistance, superheating, variable properties, and diffusion. *Int. J. Heat Mass Transfer*, **9**: 1125-1144, 1966.
- [8] H. Nagasaka, K. Yamada, M. Katoh, S. Yokobori. Heat removal tests of isolation condenser applied as a passive containment cooling system. *First Intl. Conf. on Nuclear Engineering*, Tokyo, Japan, 1: 257-263, Nov. 4-7, 1991.
- [9] E.M. Sparrow, S.H. Lin. Condensation heat transfer in the presence of a noncondensable gas. *Journal of Heat Transfer*, 430-436, 1964.
- [10] K.M. Vierow. *Behavior of Steam-Air Systems Condensing in Cocurrent Vertical Downflow*. M.S. thesis, University of CA at Berkeley, Berkeley, CA, Aug. 1990.

- [11] K.M. Vierow, J.R. Fitch, F.E. Cooke. Analysis of SBWR passive containment cooling following a LOCA. *Proceedings of Intl. Conf. on Design and Safety of Advanced Nuclear Power Plants*, Tokyo, Japan, 3: 31.2-1-31.2-7, Oct. 25-29, 1992.
- [12] K.M. Vierow, V.E. Schrock. Condensation in a natural circulation loop with noncondensable gases, Part 1 — Heat Transfer. *Proceedings of Intl. Conf. on Multiphase Flows '91*, Tsukuba, Japan, 1: 183-186, Sept. 1991.
- [13] K.M. Vierow et al. BWR passive containment cooling system by condensation-driven natural circulation. *Proceedings of First Intl. Conf. on Nuclear Engineering*, Tokyo, Japan, 1: 289-294, Nov. 4-7, 1991.

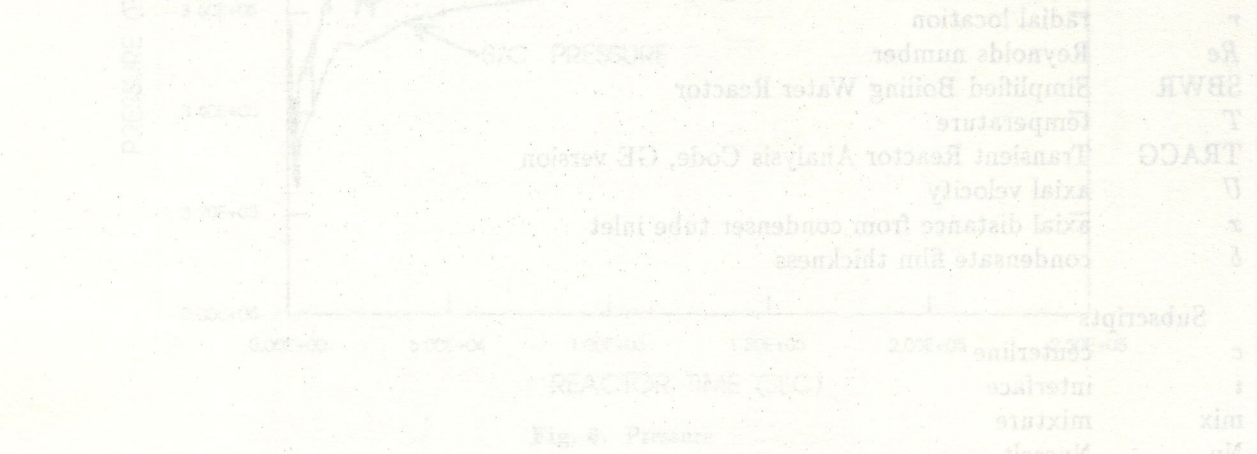


Fig. 3. Pressure vs. distance.

The condensation-driven natural circulation system is a passive safety system for BWRs. It is designed to provide cooling for the reactor core in the event of a LOCA. The system consists of a primary loop and a secondary loop. The primary loop is connected to the reactor core and the secondary loop is connected to a condenser. The condenser is cooled by a natural circulation loop of water. The system is designed to maintain the reactor core at a safe temperature and to prevent a meltdown.

REFERENCES

[1] M. Atami, I.G.M. Anderson, A.I. Yang, B.S. Spitzer. TRACG prediction of steady-state condensation heat transfer in a BWR passive containment cooling system. *Proceedings of Intl. Conf. on Design and Safety of Advanced Nuclear Power Plants*, Tokyo, Japan, 3: 31.2-1-31.2-7, Oct. 25-29, 1992.

[2] J.G.M. Anderson, J.C. Cheng. Steady-state condensation heat transfer in a BWR passive containment cooling system. *Proceedings of Intl. Conf. on Design and Safety of Advanced Nuclear Power Plants*, Tokyo, Japan, 3: 31.2-1-31.2-7, Oct. 25-29, 1992.

[3] J.G.M. Anderson et al. Steady-state condensation heat transfer in a BWR passive containment cooling system. *Proceedings of Intl. Conf. on Design and Safety of Advanced Nuclear Power Plants*, Tokyo, Japan, 3: 31.2-1-31.2-7, Oct. 25-29, 1992.

[4] V.M. Bonch-Bruyevich et al. Heat transfer from steam condensation inside vertical tubes and coils. *Heat Transfer*, 1971.

[5] V.M. Bonch-Bruyevich et al. Heat transfer from steam condensation inside vertical tubes and coils. *Heat Transfer*, 1971.

[6] V.M. Bonch-Bruyevich et al. Heat transfer from steam condensation inside vertical tubes and coils. *Heat Transfer*, 1971.

[7] W.J. Minkowicz, E.M. Sparrow. Condensation heat transfer in the presence of noncondensable inertial resistance. *Journal of Heat Transfer*, 1971.

[8] H. Nagasaka, K. Yamada, M. Katoh, S. Yokohari. Heat removal from a passive containment cooling system. *First Intl. Conf. on Nuclear Engineering*, Tokyo, Japan, 1: 289-294, Nov. 4-7, 1991.

[9] E.M. Sparrow, S.H. Lee. Condensation heat transfer in the presence of a noncondensable gas. *Journal of Heat Transfer*, 1971.

[10] K.M. Vierow. Behavior of steam-air systems condensing in a BWR passive containment cooling system. *Proceedings of Intl. Conf. on Design and Safety of Advanced Nuclear Power Plants*, Tokyo, Japan, 3: 31.2-1-31.2-7, Oct. 25-29, 1992.